Journal of Electrical and Computer Engineering Innovations
(JECEI)
Journal homepage: http://www.jecei.sru.ac.ir

Research paper

Observer-Based Fast Finite Time Robust-Adaptive Fractional Order Sliding Mode Control of DC-DC Buck Converters with Unknown Parameters

Seyyed Reza Mousavi-Aghdam *, *Milad Pourhasan*

Department of Electrical Engineering, Faculty of Engineering, University of Mohaghegh Ardabili, Ardabil, Iran.

Article Info

Article History:
Received 09 June 2025
Reviewed 15 August 2025
Revised 23 August 2025
Accepted 01 September 2025

Keywords:
Fractional-Order control
DC-DC bulk converter
Robust-Adaptive control
Sliding mode control
State-Disturbance observer
Finite time stability

*Corresponding Author's Email Address:
R.mousaviaghdam@uma.ac.ir

Abstract

Objectives: The objective of this study is to achieve fast finite-time control of DC-DC buck converters by designing a robust-adaptive terminal sliding-mode controller utilizing a fractional-order control strategy combined with a state-disturbance observer. The work begins by considering that all dynamic parameters of the converter circuit, such as resistance, capacitance, and inductance, are completely unknown due to significant uncertainties.
Methods: To formulate the stabilizing fractional-order sliding mode controller, the fractional-order sliding surface is initially presented. Given the absence of knowledge about the converter's dynamic parameters, an adaptive fractional-order finite-time sliding mode controller is developed to ensure the finite-time stability of the system and to achieve rapid convergence of the converter voltage to the prescribed reference value in the presence of parameters uncertainties and external disturbances. To estimate unknown varying parameters in the converter, an adaptive law is additionally designed. Furthermore, a high-speed observer is incorporated to estimate both external disturbances and the state variables affecting the system. An analysis is also presented to find the maximum allowable sampling time based on the controller parameters.
Results: The closed-loop system stability is validated through the application of the extended Lyapunov method. Importantly, the proposed method ensures that the output voltage of the converter reaches its desired value within a finite time, taking external disturbances into account as well as operating with unknown parameters, and also, without direct feedback from voltage or current measurements. Ultimately, simulation results along with some enhanced robustness analysis are presented to demonstrate the effectiveness of the proposed control approach.
Conclusion: The innovative controller based on fractional-order sliding mode control in senseless DC-DC buck converters is considered. The goal is to converge the output voltage to the desired value in finite time considering that all of the converter dynamic parameters are unknown and system is exposed to external disturbances. Chattering is reduced using a new technique, and the maximum allowable sampling time is also obtained. The results validate the suitability of the proposed technique, especially in overcoming uncertainties and disturbances without requiring voltage/current measurements.

How to cite this paper:
S. R. Mousavi-Aghdam, M. Pourhasan, "Observer-based fast finite time robust-adaptive fractional order sliding mode control of DC-DC Buck converters with unknown parameters," J. Electr. Comput. Eng. Innovations, 14(1): 181-196, 2026.
DOI: 10.22061/jecei.2025.11939.843
URL: https://jecei.sru.ac.ir/article_2409.html

Introduction

Power converters use simple on-off switches to control their operation [1], [2]. Among these, buck converters are a widely recognized topology. With the continuous progress in various DC power supply technologies, buck converters have become integral in numerous applications, including photovoltaic systems [3], electric vehicles [4], and smart grid networks [5]. These uses require precise voltage control and good disturbance rejection. However, despite their extensive use, achieving optimal performance in these nonlinear systems under disturbance conditions remains a significant challenge [6]. Control is challenging because converters are nonlinear and sensitive to load/input changes and external disturbances. Consequently, there is a growing interest in improving the control performance of buck converter systems. PID controllers [7], [9] are popular because they're simple to implement. The integral part of the PID controller helps ensure the system's convergence. But they struggle with fast-changing disturbances. Specifically, PID controllers tend to perform poorly in the presence of uncertainties related to load resistance and input voltage variations. To overcome these challenges, a variety of nonlinear control techniques have been developed, such as model predictive control [10], [12], robust control [13], [14], adaptive control [15], [16], back-stepping control [17], [18], active disturbance rejection control [19], [20] and sliding mode control (SMC) [21], [29]. Each of these strategies aims to improve the performance of buck converters from different perspectives. SMC works particularly well for certain disturbance types. As mentioned earlier, in DC buck converters, control variables are constrained to discrete values. Consequently, SMC is not only a preferred theoretical approach but also a practical choice, supported by a wide range of automatic control designs for power converters in various applications.

In modern power converter control techniques, pulse-width modulation (PWM) methods are commonly used. However, a key drawback of PWM-based systems, including those that employ sliding mode control (SMC), is the development of unwanted oscillations with finite amplitude and frequency. These oscillations arise due to unmodeled dynamics or the effects of discrete-time implementations. This 'chattering' effect reduces precision and may damage components [30],[32]. Moreover, SMC can introduce frequency variations that may be undesirable in specific applications [33], [36].

In [21], a sliding mode algorithm is modified to enhance the performance of switch-mode converters. The presence of mismatched disturbances can lead to a steady-state error in the output voltage of the converter. To address this, in [22], [23], an extended state observer (ESO) is incorporated into SMC to estimate and handle these mismatched disturbances. However, this method only ensures asymptotic tracking of the output voltage. To further improve dynamic performance, a disturbance observer with finite-time convergence properties (FTDO) is integrated into nonsingular terminal sliding mode control, enabling finite-time control of converter systems [24]. Despite this, the discontinuous nature of the control law and the use of large switching gains can still lead to chattering, which may result in voltage ripples. Additionally, applying this approach to higher-order converter systems introduces further challenges. In [16], an adaptive algorithm is utilized to adjust the sliding mode gain, resulting in better chattering reduction. Furthermore, the approaches in [25], [26] propose high-order sliding mode control as a means to further reduce chattering. However, this introduces increased complexity in tuning the controller parameters.

As far as the authors are aware, prior studies have not investigated the finite-time stability of DC-DC buck converters in the face of external perturbations and uncertain modeling, assuming that fundamental dynamic characteristics such as resistance, capacitance, and inductance remain unspecified.

In this work, the unknown parameters of the DC-DC buck converter are estimated using a fractional-order sliding-mod control scheme with finite-time convergence, coupled with a stable adaptation law. This ensures that the converter’s output voltage converges within a finite, preassigned period. However, establishing finite-time stability becomes particularly difficult when adaptive laws are used to estimate the dynamic parameters. The paper introduces a novel control scheme designed to maintain finite-time stability despite the use of adaptive laws.

However, due to potential faults in the sensors of a bulk converter, it is often not possible to measure the exact values of the converter’s variables, such as its voltage and current. To address this issue, this paper proposes a state and disturbance observer that can simultaneously estimate both the converter's voltage/current and the unknown disturbances affecting the system. The key contributions and innovations of this paper are summarized as follows :(1) formulation of an original fractional-order sliding surface and implementation of a terminal fractional-order sliding-mode controller for a DC–DC buck converter, (2) Fast finite-time convergence of the converter output to the desired voltage is achieved, even when the dynamic parameters of the converter are completely unknown, (3) A new method is introduced to demonstrate the finite-time convergence of the output voltage in the presence of stable adaptive laws, and (4) A state-disturbance observer is designed to estimate both the

converter's voltage/current and its unknown disturbances simultaneously.

In essence, the primary innovation of this paper lies in the design of a new controller that ensures the convergence of the DC-DC buck converter's output voltage to the desired value within a predetermined finite time, rather than in infinite time, as typically achieved in asymptotic stability. This approach accounts for real-world, practical constraints that have not been previously addressed in the literature. It is important to note that with the proposed method, the finite-time convergence of the converter's output voltage to its desired value is achieved even in the presence of external disturbances, with completely unknown parameters, and without access to voltage and current measurements for feedback.

While existing control methods have advanced buck converter performance, they face fundamental limitations in practical scenarios involving complete parametric uncertainty and sensor failures. This work bridges this gap by developing a control framework that simultaneously addresses: (1) complete ignorance of dynamic parameters (R, L, C values), (2) operation without current/voltage measurements, (3) rejection of external disturbances, while guaranteeing (4) finite-time convergence - a crucial requirement for safety-critical applications where asymptotic stability is insufficient. The proposed architecture uniquely combines fractional-order sliding modes with adaptive parameter estimation and disturbance observation to achieve these objectives.

Study Background

Fractional calculus, an extension of classical differentiation and integration to non-integer orders, has gained traction in control engineering due to its superior modeling capabilities. Different fractional differentiation definitions exist, such as Grünwald-Letnikov, Riemann-Liouville, and Caputo, which offer improved system dynamics representation [37], [39].

$$ {}_aD_t^{\alpha} = \begin{cases} \dfrac{d^{\alpha}}{dt^{\alpha}} & ,\ R(\alpha) > 0 \\ 1 & ,R(\alpha) = 0 \\ \int_a^t (d\tau)^{-\alpha} & ,R(\alpha) < 0 \end{cases} \tag{1} $$

where α represents the initial conditions, and, under a fractional-order framework, these can take the form of a constant or a complex number.

$$ {}_aD_t^{\alpha} f(t) = \lim_{h\to 0} \frac{1}{h^{\alpha}} \sum_{j=0}^{[(t-\alpha)/h]} (-1)^j \binom{\alpha}{j} f(t-jh)_a \tag{2} $$

where $[.]$ represents the floor operator. The Caputo definition is provided in [37]-[39].

$$ {}_aD_t^{\alpha} f(t) = \frac{1}{\Gamma(n-\alpha)} \frac{d^n}{dt^n} \int_a^t \frac{f(\tau)}{(t-\tau)^{\alpha-n+1}} d\tau \tag{3} $$

where $(n-1<\alpha<n)$ and $\Gamma(x)$ denotes the Gamma function. Now, let us consider the following two lemmas:

Lemma 1 [37], [40]: Let $V(x)$ be a Lyapunov function, where V_0 representing its initial condition. It follows that:

$$ \dot{V}(x) + \alpha V(x) + \beta V^{\gamma}(x) \le 0 \tag{4} $$

where $\alpha, \beta > 0$ and $0 < \gamma < 1$. Consequently, the Lyapunov function reaches zero within a finite interval T, as described by the following:

$$ T \le \alpha^{-1}(1-\gamma)^{-1} \ln(1+\alpha\beta^{-1}V_0^{1-\gamma}) \tag{5} $$

Lemma 2 [37], [40]: Let us investigate the following equation:

$$ \dot{x} + kD^{\lambda-1}[sig(x)^a] = 0 \tag{6} $$

where $x \in R^n, 0 \prec a, \lambda \prec 1, k = diag(k_i)$ is a constant positive matrix in which $k_i \in R^+ \ i = 1,2,...,n$ and $sig(x)^a$ is defines as:

$$ sig(x)^a = [|x_1|^{a_1} sign(x_1), ..., |x_n|^{a_n} sign(x_n)]^T \tag{7} $$

Thus, the states x and $\dot{x}$ will settle within a small vicinity of the origin, enclosed by a sufficiently small radius $\Delta = \dfrac{\|\varepsilon\|}{\lambda_{\min}(k_i)}$ in finite time [40].

The next section outlines the problem definition, system description, and the objective of this paper.

Converter System Details

This paper examines the DC-DC buck converter depicted in Fig. 1.

$$ \begin{cases} \dfrac{dv_o(t)}{dt} = \dfrac{1}{C} i_L(t) - \dfrac{1}{C} i_o(t) - \dfrac{1}{r_C C} v_o(t) \\ \dfrac{di_L(t)}{dt} = \dfrac{1}{L} m(t) V_{in}(t) - \dfrac{1}{L} r_L i_L(t) - \dfrac{1}{L} v_o(t) \end{cases} \tag{8} $$

where v_o represents the average output capacitor voltage, $i_L(t)$ denotes the average inductor current, and $m(t)$ corresponds to the PWM input signal. As illustrated in Fig. 1, the DC-DC buck converter circuit consists of a PWM-controlled MOSFET switch, a DC voltage source (V_{in}), a diode, an inductor (L), accompanied by its parasitic resistance (r_L), a capacitor, a parallel resistor (r_c), and a load, which is assumed to be a resistor (R).

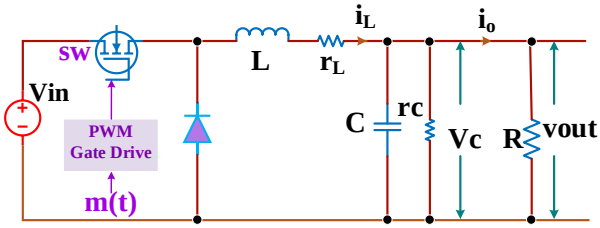

Fig. 1: Schematic diagram of a DC-DC buck converter.

It is worth noting that the parallel resistor serves to discharge the capacitor as a protective measure [32]. Additionally, this resistor can be regarded as a source of system parameter variation.

Define the following state variables:

$$\begin{cases} x_1(t) = v_o(t) \\ x_2(t) = i_L(t) \\ y(t) = x_1(t) \end{cases} \tag{9}$$

considering $u(t) = m(t), i_o = \frac{1}{R} v_o$, then (8) can be written as follows:

$$\begin{cases} \dot{x}_1(t) = \frac{1}{C} x_2 - \frac{1}{RC} x_1 - \frac{1}{r_C C} x_1 \\ \dot{x}_2(t) = \frac{1}{L} V_{in} u - \frac{1}{L} r_L x_2 - \frac{1}{L} x_1 \\ y(t) = x_1 \end{cases} \tag{10}$$

Thus, the state-space representation of system (9) can be expressed as follows:

$$\begin{bmatrix} \dot{x}_1 \\ \dot{x}_2 \end{bmatrix} = \begin{bmatrix} -(\frac{1}{RC} + \frac{1}{r_C C}) & \frac{1}{C} \\ -\frac{1}{L} & -\frac{r_L}{L} \end{bmatrix} \begin{bmatrix} x_1 \\ x_2 \end{bmatrix} + \begin{bmatrix} 0 \\ \frac{1}{L} V_{in} \end{bmatrix} u$$
$$y = \begin{bmatrix} 1 & 0 \end{bmatrix} \begin{bmatrix} x_1 \\ x_2 \end{bmatrix} \tag{11}$$

The standard state-space model can be obtained as follows:

$$\begin{aligned} \dot{x} &= Ax + Bu \\ y &= Cx \end{aligned} \tag{12}$$

where the parameters are defined as follows:

$$A = \begin{bmatrix} -(\frac{1}{RC} + \frac{1}{r_C C}) & \frac{1}{C} \\ -\frac{1}{L} & -\frac{r_L}{L} \end{bmatrix}, \quad B = \begin{bmatrix} 0 \\ \frac{1}{L} V_{in} \end{bmatrix}$$
$$C = \begin{bmatrix} 1 & 0 \end{bmatrix} \tag{13}$$

in which $x(0) \in R^n$ is the initial condition vector, $A \in R^{n \times n}$ is the state matrix and $B \in R^{n \times 1}$ s the matrix of input coefficients, representing the system dynamics. Here, $u \in R$ serves as the input, $y \in R$ represents the output, and $C \in R^{1 \times n}$ specifies the output matrix.

The goal of controlling a DC-DC buck converter is to adjust the output voltage to a desired level as quickly as possible, despite unknown load variations. In both industrial applications and research, two primary methods have been employed to solve this issue: voltage control and current control. In the voltage control method, voltage error is used to set the duty cycle, which in turn directly sets the duty cycle for the PWM modulator. On the other hand, the current control method involves measuring both the inductor current and the output voltage. Uses cascaded loops (outer voltage, inner current) for the inner current control loop.

The aim of this paper is to propose a reliable adaptive controller capable of regulating the output voltage with high precision and fast response, even under the presence of model uncertainties and external disturbances. To achieve this, we develop a finite-time robust adaptive fractional-order sliding-mode control (FRAFSMC) system, which incorporates adaptive regulation laws. We start by formally defining finite-time stability, as presented in [41], [42].

Definition (time-bounded stability): Consider the system

$$\dot{x} = h(x), \; x_0 = x(0) \tag{14}$$

which the vector field, is defined as $h : R^n \to R^n$ and the state vector is $x \in R^n$. Assume the origin of system (14), $x = 0$ is stable asymptotically. The origin is stable in finite time (FTS) if, $\forall x_0 \in B_\delta \setminus \{0\}$, $\exists x(t, x_0)$ of system (14) reaches the origin at a specific finite time and stays there for all future times, such that $t \geq T(x_0)$, where $T : B_\delta \setminus \{0\} \to (0, \infty)$ is the time required to settle, which is dependent on the initial state x_0.

Now, by taking the derivative of $\dot{x}_1$ in (10) we obtain

$$\ddot{x}_1(t) = \frac{1}{C} \dot{x}_2(t) - \frac{1}{RC} \dot{x}_1(t) - \frac{1}{r_C C} \dot{x}_1(t) \tag{15}$$

By substituting $\dot{x}_1, \dot{x}_2$ form (10) into (15) we can obtain the following relationship (For convenience, the notation t, representing time, is omitted throughout the remainder of the paper).

$$\ddot{x}_1 = \frac{1}{LC} V_{in} u - \frac{1}{LC} r_L x_2 - \frac{1}{LC} x_1 - (\frac{1}{RC} + \frac{1}{r_C C}) \dot{x}_1 \tag{16}$$

Assume the functions $f(x_1, x_2, \dot{x}_1), g(x_1, x_2, \dot{x}_1)$ as follows:

$$\begin{aligned} f(x_1, x_2, \dot{x}_1) &= -\frac{1}{LC} x_1 - \frac{1}{LC} r_L x_2 - (\frac{1}{RC} + \frac{1}{r_C C}) \dot{x}_1 \\ g(x_1, x_2, \dot{x}_1) &= \frac{1}{LC} V_{in} \end{aligned} \tag{17}$$

So, the nonlinear dynamic system is as follows

$$\begin{aligned} \ddot{x}_1 &= f(x_1, x_2, \dot{x}_1) + g(x_1, x_2, \dot{x}_1) u \\ y &= x_1 \end{aligned} \tag{18}$$

In reality, dynamic systems are frequently subjected to model uncertainties. As a result, many traditional controllers face challenges in effectively regulating such systems when uncertainties, disturbances, or un-modeled dynamics are present.

Hence, we assume the following assumption holds true in this paper:

Assumption: It is presumed that considerable parameter uncertainty causes the nonlinear affine system's dynamic functions in (16) to remain unspecified. Based on Assumption, the dynamic model of the system with uncertainty can be represented as follows:

$$\ddot{x}_1 = \hat{f}(x_1, x_2, \dot{x}_1) + \hat{g}(x_1, x_2, \dot{x}_1)u$$
$$y = x_1 \quad (19)$$

where $\hat{f}(x_1, x_2, \dot{x}_1)$ and $\hat{g}(x_1, x_2, \dot{x}_1)$ denote the estimated dynamic functions of the system. The goal of this study is to formulate a fractional-order adaptive sliding-mode controller that guarantees finite-time convergence of $y(t)$ to $y_d(t)$, despite complete uncertainty about the DC–DC buck converter's dynamics (Assumption). In this framework, the system's dynamic parameters are approximated using an adaptive law, with the objective of nullifying the tracking error and driving it to zero regardless of the system's starting state.

Design of Adaptive Fractional-Order Terminal Sliding Mode Control

A. Reformulation of the Converter Model

Sliding Mode Control (SMC) is a resilient nonlinear control method grounded in Lyapunov theory, employing a first-order framework to simplify an nth-order nonlinear system with uncertainties. The design process for sliding mode control involves two primary steps: The first step is to define a switching function that ensures the system follows the desired sliding motion, meeting the control objectives. The second step is to choose a control law that enforces and sustains the sliding mode. This section introduces the stabilization method utilizing fractional-order control (FOC) for designing the sliding mode controller for the DC-DC buck converter. The system dynamics in (18) can be expressed as follows:

$$\ddot{x}_1 = F + Gu + L(x_1, x_2, \dot{x}_1)$$
$$y = x_1 \quad (20)$$

where F and G are known constants, $u(t)$ denotes the control input signal that requires determination, and $L(x_1, x_2, \dot{x}_1)$ is defined as follows:

$$L(x_1, x_2, \dot{x}_1) = f(x_1, x_2, \dot{x}_1) - F$$
$$+(g(x_1, x_2, \dot{x}_1) - G)u \quad (21)$$

Here, $L(x_1, x_2, \dot{x}_1)$ represents the uncertain part of the system model. It can be a regressor structure in terms of the unknown dynamic parameters as follows:

$$L(x_1, x_2, \dot{x}_1) = \left(-\frac{1}{LC}x_1 - \frac{1}{LC}r_L x_2 - \left(\frac{1}{RC} + \frac{1}{r_C C}\right)\dot{x}_1 - F\right)$$
$$+\left(\frac{1}{LC}V_{in} - G\right)u \quad (22)$$

Therefore, $L(x_1, x_2, \dot{x}_1)$ can be written as a linear expression involving the unknown system parameters $\theta \in R^m$ and the known regressor matrix $Y(x_1, x_2, \dot{x}_1) \in R^{1\times m}$ as shown below:

$$Y(x_1, x_2, \dot{x}_1) = \begin{bmatrix} -x_1 & -x_2 & -\dot{x}_1 & u & -F \end{bmatrix},$$
$$\theta = \begin{bmatrix} \frac{1}{LC} & \frac{r_L}{LC} & \frac{1}{RC} + \frac{1}{r_C C} & \frac{1}{LC}V_{in} - G & 1 \end{bmatrix}^T \quad (23)$$

Hence, the regressor representation of $L(x_1, x_2, \dot{x}_1)$ is as follows:

$$L(x_1, x_2, \dot{x}_1) = Y(x_1, x_2, \dot{x}_1)\theta \quad (24)$$

B. Formulating the Fractional-Order Sliding Surface and Convergence Law

Let there be a tracking error, denoted as $\tilde{y} = y_d - y \in R$. between the desired and actual outputs of the system. To guarantee finite-time stability of the tracking error in the dynamic model (18), the fractional-order sliding mode manifold is defined as follows:

$$s = \dot{\tilde{y}} + kD^{\beta-1}[sig(\tilde{y})^{\alpha}] \quad (25)$$

where $sig(\tilde{y})^{\alpha} = |\tilde{y}|^{\alpha} sign(\tilde{y})$ with $0 < \alpha, \beta < 1$ and k is a specified positive constant. The sliding mode of the system, characterized by $s = 0, \dot{s} = 0$ rdenotes the system's trajectory along the sliding surface. Under this condition, the tracking error $\dot{\tilde{y}} + kD^{\beta-1}[sig(\tilde{y})^{\alpha}] = 0$ evolves according to the system's dynamics. Furthermore, the results derived from Lemma 2 suggest that the tracking errors will eventually settle within a constrained region near the system's zero state.

The purpose of this control scheme is to bring the system's dynamics onto the sliding surface in an allotted finite time. To ensure a brisk approach to zero before that interval elapses, the following fractional‑order reaching law is offered [8], [29]:

$$\dot{s} = -\rho s - \mu |s|^{\lambda} sign(s)$$
$$\rho, \mu \in R^{+}$$
$$0 < \lambda < 1 \quad (26)$$

where $\rho, \mu \in R$ are positive constant and $0 < \lambda < 1$. In the following subsection, it is demonstrated that, utilizing the reaching law from the sliding surface attains the zero state within a predetermined finite time (24).

C. Robust Adaptive Controller Based on Fractional-order Terminal Sliding-mode Control

Assume that $\hat{\theta}$ denotes the approximated dynamic parameters θ in equation (24). Considering the sliding surface defined in (25) and the fractional-order approach for the reaching law in (26), the fractional-order sliding mode controller is formulated as follows to ensure convergence to the desired trajectory within a finite time for a nonlinear input-affine system, with the governing dynamic relations outlined in equations (18)-(24):

$$u(t) = (G)^{-1}\left(-F - Y\hat{\theta} + \tau(t)\right) \quad (27)$$

where τ is below

$$\tau(t) = \ddot{y}_d + kD^{\beta}[sig(\tilde{y})^{\alpha}] + \rho s + \mu sig(s)^{\lambda} \quad (28)$$

and $\hat{\theta}$ in (27) is obtained based on the adaptive rule outlined below:

$$\dot{\hat{\theta}} = -\Gamma Y^T s \tag{29}$$

where $\Gamma \in R^{m\times m}$ denotes an arbitrary positive-definite matrix serving as the adaptive gain. The ensuing establishes that the closed-loop system defined by (18)-(29) achieves finite-time stability under the proposed adaptive sliding-mode controller. This theorem represents the core contribution of this paper.

Theorem 1: By assuming the nonlinear model in (18), the fractional-order adaptive sliding-mode control law described in (27)-(29) guarantees that $y(t)$ converges to the reference trajectory $y_d(t)$ within a finite time.

Proof: Utilizing (20) and taking the second derivative of the output in (18) yields the following result.

$$\begin{aligned}\ddot{y} = \ddot{x}_1 &= \left(F + Gu + L(x_1, x_2, \dot{x}_1)\right) \\ &= F + Gu + L\end{aligned} \tag{30}$$

By replacing the control law from (27) into the altered dynamic equation in (30) and including (24), the following expression is obtained:

$$\ddot{y} = -Y\hat{\theta} + \tau(t) + Y\theta = \tau(t) - Y\tilde{\theta} \tag{31}$$

where $\tilde{\theta} = \hat{\theta} - \theta$ represents the discrepancy in the estimated dynamic parameters. Now, by substituting τ from (28) into (31), the following expression is derived

$$\ddot{\tilde{y}} + kD^{\beta}[sig(\tilde{y})^{\alpha}] + \rho s + \mu sig(s)^{\lambda} - Y\tilde{\theta} = 0 \tag{32}$$

Now, let's consider the following candidate for a positive definite Lyapunov function

$$V = \frac{1}{2}s^2 + \frac{1}{2}\tilde{\theta}^T\Gamma^{-1}\tilde{\theta} \tag{33}$$

Differentiating V with respect to time results

$$\dot{V} = s\dot{s} + \tilde{\theta}^T\Gamma^{-1}\dot{\tilde{\theta}} \tag{34}$$

By applying (26) and noting that $\dot{\tilde{\theta}} = \dot{\hat{\theta}}$ remains constant (because the dynamic parameters do not change), we obtain:

$$\dot{V} = s\left(\ddot{\tilde{y}} + kD^{\beta}[sig(\tilde{y})^{\alpha}]\right) + \tilde{\theta}^T\Gamma^{-1}\dot{\hat{\theta}} \tag{35}$$

By substituting the dynamic error from (32) into (35), we obtain:

$$\dot{V} = s\left(-\rho s - \mu sig(s)^{\lambda} + Y\tilde{\theta}\right) + \tilde{\theta}^T\Gamma^{-1}\dot{\hat{\theta}} \tag{36}$$

By implementing the adaptive law from (29) into (36), we derive:

$$\begin{aligned}\dot{V} &= -\rho s^2 - s\mu sig(s)^{\lambda} + sY\tilde{\theta} - \tilde{\theta}^T Y^T s \\ &= -\rho s^2 - s\mu sig(s)^{\lambda}\end{aligned} \tag{37}$$

Considering the definition of $sig(s)^{\lambda}$ as $sig(s)^{\lambda} = |s|^{\lambda} sign(s)$ and noting that $\left(|s|^2\right)^{1+\lambda} \le \left(|s|^{1+\lambda}\right)^2$ holds for $0 < \lambda < 1$ [24], hence, the upper bound on $\dot{V}$ in (37) can be expressed as follows:

$$\dot{V} \le -\rho\|s\|^2 - \mu\|s\|^{1+\lambda} \tag{38}$$

The time derivative of the Lyapunov function in (38) is non-positive. By introducing $\tilde{w}(t) = \rho\|s\|^2 + \mu\|s\|^{1+\lambda}$ and performing integration on both sides of (38), it can be inferred that $V(0) \ge V(t) + \int_0^t \tilde{w}(\lambda)d\lambda$. From this relationship, it can be concluded that $\infty > V(0) \ge \lim_{t\to\infty}\int_0^t \tilde{w}(\lambda)d\lambda$. Therefore, based on Barbalat's Lemma (see [43]), $\tilde{w}(t)$ and, consequently, $s(t)$ will approach zero as $t \to \infty$. As a result, the system described in (18), with the control input given by (27) and the adaptive law in (29), exhibits asymptotic stability, as confirmed by (26). The $s(t)$ convergence to zero occurs within a finite time, as will be demonstrated in the following subsection.

D. Analysis of Finite-time Stability

Consequently, the system modeled by (18), when driven by the control input specified in (27), the term $s(t)$ will asymptotically approach zero, while the tracking deviations $\tilde{y}$ will eventually settle within a restricted area around the origin, and this convergence will occur within a finite duration (denoted as $T_{\tilde{x}}$).

In this section, the goal is to demonstrate that the system will converge to the sliding surface ($s(t) = 0$) within a finite time, denoted as T_s. Consequently, it can be concluded that all tracking errors in the controlled system will ultimately be eliminated within a predetermined time interval, $T_{final} = T_{\tilde{x}} + T_s$. To determine T_s let us introduce the following new Lyapunov function:

$$V_s = \frac{1}{2}s^2 \tag{39}$$

Remark 1. It is important to highlight that the Lyapunov function defined in (33) can only confirm the asymptotic stability of the affine system, not its finite-time stability. A necessary step in establishing finite-time stability is to prove that the sliding surface itself decays to zero within a finite interval. Lemma 2 then ensures that, once the sliding surface is reached, the associated error dynamics are guaranteed to exhibit finite-time stability.

By differentiating with respect to time and utilizing (25), we obtain:

$$\dot{V}_s = s\left(\ddot{\tilde{y}} + kD^{\beta}[\mathrm{sgn}(\tilde{y})^{\alpha}]\right) \tag{40}$$

Substituting (32) into (40) yields

$$\dot{V}_s = -s\left(\rho s + \mu sig(s)^{\lambda} - \varepsilon\right) \tag{41}$$

where $\varepsilon = Y\tilde{\theta}$ denotes the remaining deviation vector once control is enacted. As stated in Theorem 1, $\tilde{\theta}$ remains within finite limits, which implies that ε also

remains confined, guaranteeing $|\varepsilon| \le \eta, \eta > 0$. Equation (39) may be expressed in either of these two equivalent formulations:

$$\dot{V}_s = -s\left(\left(\rho + \varepsilon s^{-1}\right)s + \mu sig(s)^{\lambda}\right) \quad (42)$$

$$\dot{V}_s = -s\left(\left(\rho + (\mu + \varepsilon(sig(s)^{\lambda})^{-1})sig(s)^{\lambda}\right)\right) \quad (43)$$

Consequently, equation (42) can initially be simplified as follows:

$$\dot{V}_s = -s\left(\bar{\rho}s + \bar{\mu}sig(s)^{\lambda}\right) = -s\bar{\rho}s - s\bar{\mu}sig(s)^{\lambda} \quad (44)$$

where $\bar{\rho} = \rho + \varepsilon s^{-1}$ and $\bar{\mu} = \mu$. In a similar manner to what is presented in (38), we obtain:

$$\dot{V}_s \le -\bar{\rho}\|s\|^2 - \bar{\mu}\|s\|^{1+\lambda} \quad (45)$$

Now, by utilizing (39) and substituting the $\|s\| = \sqrt{2V_s}$ into (45), we obtain

$$\dot{V}_s \le -2\bar{\rho}V_s - 2^{1+\lambda/2}\bar{\mu}V_s^{1+\lambda/2} \quad (46)$$

By employing the first lemma, a straightforward comparison between (44) (which may alternatively be expressed as $\dot{V}_s + 2\bar{\rho}V_s + 2^{1+\lambda/2}\bar{\mu}V_s^{1+\lambda/2} \le 0$) and (4) clearly indicates that, in a similar manner to how $V(x)$ in (4) reaches zero within a finite duration, determined by the settling time in (5), V_s will also approach zero in a finite time, and with the settling time defined by:

$$T_s \le \frac{1}{\bar{\rho}(1-\lambda)}\ln\left(1 + \frac{2\bar{\rho}V_s^{1-\lambda/2}}{2^{1+\lambda/2}\bar{\mu}}\right) \quad (47)$$

Hence, the system will reach $\|s\| \le \|\varepsilon\|/\bar{\rho}$ in a finite duration. In a similar manner, applying the expression in (41) leads to the system converging to $\|s\| \le \left(\|\varepsilon\|/\bar{\mu}\right)^{1/\lambda}$ within a finite time span. As a result, the system trajectories will converge to a closed ball centered at $s(t) = 0$ within a finite time, as follows:

$$\begin{aligned} &\|s\| \le \Omega = \min(\Omega_1, \Omega_2) \\ &\Omega_1 = \|\varepsilon\|/\bar{\rho} \\ &\Omega_2 = \left(\|\varepsilon\|/\bar{\mu}\right)^{1/\lambda} \end{aligned} \quad (48)$$

Therefore, the errors tracking $\tilde{y}$ will approach zero within a finite time $T_{final} = T_{\tilde{y}} + T_s$, as shown in (45), where T_s is defined in (45), and $T_{\tilde{y}}$ represents the finite settling time under the sliding mode condition ($s(t) = 0$)

E. Analysis of Chattering

The main issue when applying sliding-mode control in practical scenarios is chattering, which refers to unwanted oscillations with small amplitude and high frequency. This is typically caused by the discontinuous nature of the sign function in the control input. To reduce or eliminate chattering, various techniques have been suggested. In this work, a pseudo-sliding function is employed to minimize chattering. Specifically, the sign function $\rho\,\mathrm{sgn}(s), \rho > 0$ is estimated using the following function:

$$\rho\,\mathrm{sgn}(s) \cong \frac{\rho^2 s}{\rho\|s\| + \sigma(t)} \quad (49)$$

where $\sigma(t) \succ 0$ is a positive and bounded function, ensuring that $\int_0^{\infty}\sigma(t)dt \prec \infty$. For instance,

$$\sigma(t) = \frac{1}{1+t^n}, \quad n \ge 2 \quad (50)$$

One must underscore that the main advantage of this approach over conventional methods lies in the fact that, distinct from alternative schemes, the procedure outlined in (49) to generate a smooth surrogate of the signum function rapidly approaches the true signum function, thus obviating the need for any additional approximation.

Sampling Time Analysis

In a DC-DC bulk converter controlled by a fractional-order sliding mode controller (FOSMC), sampling time significantly impacts stability. Increasing the sampling time (i.e., decreasing the sampling frequency) can lead to instability or degraded performance, while a smaller sampling time generally improves stability and tracking accuracy. This is because a longer sampling time introduces a delay in the feedback loop, potentially causing the controller to overcorrect and leading to oscillations or even instability. In this section a mathematical analysis is presented to obtain the maximum allowable sampling time in the proposed fractional order sliding mode controller.

To ensure stable digital implementation of the proposed controller, consider the maximum allowable sampling interval as $\tau_{\max}$. The sliding surface in (25) can be written as:

$$s = \dot{\tilde{y}} + kD^{\beta-1}[sig(\tilde{y})^{\alpha}] = \dot{\tilde{y}} + kD^{\beta-1}\left[|\tilde{y}|^{\alpha}\,\mathrm{sign}(\tilde{y})\right] \quad (51)$$

where $0 < \alpha, \beta < 1$ are the fractional exponents, and k is a positive constant. Also, the reaching law is given by follows as in equation (26) of paper:

$$\dot{s} = -\rho s - \mu|s|^{\lambda}\,sign(s), \quad \rho, \mu \in R^+, \quad 0 < \lambda < 1 \quad (52)$$

Now, the Stability Condition Derivation is presented in some steps:

1. Discretization:

Using forward Euler discretization with sampling interval τ the reaching law becomes:

$$\frac{s_{n+1} - s_n}{\tau} = -\rho s_n - \mu|s_n|^{\lambda}\,\mathrm{sign}(s_n). \quad (53)$$

Rearrange (53) to obtain the discrete-time dynamics results

$$s_{n+1} = s_n(1-\rho\tau) - \mu\tau \mid s_n \mid^{\lambda} \operatorname{sign}(s_n) \tag{54}$$

2. Stability Condition

To ensure stability and finite-time convergence, the discrete-time system must satisfy both Contraction condition $\mid s_{n+1} \mid \lhd \mid s_n \mid$ for all $s_n \neq 0$ and Sign preservation $\operatorname{sign}(s_{n+1}) = \operatorname{sign}(s_n)$. Now, Substitute s_{n+1} from (54) in this inequality results:

$$\mid s_n(1-\rho\tau) - \mu\tau \mid s_n \mid^{\lambda} \operatorname{sign}(s_n) \mid \lhd \mid s_n \mid . \tag{55}$$

Divide (55) by $\mid s_n \mid$ (since $s_n \neq 0$) results

$$\mid (1-\rho\tau) - \mu\tau \mid s_n \mid^{\lambda-1} \mid < 1. \tag{56}$$

3. Practical Upper Bound

The worst-case scenario occurs when $\mid s_n \mid$ is smallest (near the sliding surface). Firstly, to prevent divergence and from above inequality, the sampling time must ensure

$$1-\rho\tau-\mu\tau \mid s_n \mid^{\lambda-1} > -1. \tag{57}$$

Now, linearizing near $s_n = 0$ with $\mid s_n \mid \approx \varepsilon$ and therefore approximating $\mid s_k \mid^{\lambda-1} \approx \varepsilon^{\lambda-1}$, the stability condition in (57) becomes

$$1-\rho\tau-\mu\tau\varepsilon^{\lambda-1} > -1. \tag{58}$$

which easily results

$$\tau < \frac{2}{\rho + \mu\varepsilon^{\lambda-1}} \tag{59}$$

Therefore, the maximum allowable sampling interval can be obtained as follows

$$\tau_{\max} = \frac{2}{\rho + \mu\varepsilon^{\lambda-1}} \tag{60}$$

3. Practical Implications

It should note that the fractional-order term $D^{\beta-1}[sig(\tilde{y})^{\alpha}]$ is sliding surface, does not directly affect $\tau_{\max}$ as it operates on the error $\tilde{y}$ rather than the sliding surface s. However, it indirectly improves the allowable τ by:

a) Smoothing high-frequency oscillations in $\tilde{y}$, reducing chattering.

b) Attenuating abrupt changes in s, thereby relaxing the sampling constraint.

Also, it should be noted that the maximum bound $\tau_{\max}$ is determined primarily by ρ, μ and λ from the reaching law. Using the example values of these parameters as in simulation results, the maximum sampling time is calculated as $\tau_{\max} = 0.4ms$

Also, please note that a conservative choice can be $\tau \leq \tau_{\max}/2$ to account for computational delays and unmodeled dynamics.

As conclusion, the sampling time analysis confirms that the proposed controller maintains stability under practical digital implementation. The fractional-order error term enhances robustness without tightening the sampling constraints, while the reaching law parameters govern the fundamental limit for τ.

State-disturbance Observer Design

Now, consider that the system described in (10) is impacted by an external disturbance. In this case, (10) can be reformulated as follows:

$$\begin{cases} \dot{x}_1(t) = \dfrac{1}{C}x_2 - \dfrac{1}{RC}x_1 - \dfrac{1}{r_C C}x_1 + d_1 \\ \dot{x}_2(t) = \dfrac{1}{L}V_{in}u - \dfrac{1}{L}r_L x_2 - \dfrac{1}{L}x_1 + d_2 \\ y(t) = x_1 \end{cases} \tag{61}$$

where $d_1, d_2 \in R$ represent the disturbances. Thus, the state-space model accounting for the external disturbances is expressed as follows:

$$\begin{bmatrix} \dot{x}_1 \\ \dot{x}_2 \end{bmatrix} = \begin{bmatrix} -(\dfrac{1}{RC} + \dfrac{1}{r_C C}) & \dfrac{1}{C} \\ -\dfrac{1}{L} & -\dfrac{r_L}{L} \end{bmatrix} \begin{bmatrix} x_1 \\ x_2 \end{bmatrix} + \begin{bmatrix} 0 \\ \dfrac{1}{L}V_{in} \end{bmatrix} u + \begin{bmatrix} d_1 \\ d_2 \end{bmatrix}$$
$$y = \begin{bmatrix} 1 & 0 \end{bmatrix} \begin{bmatrix} x_1 \\ x_2 \end{bmatrix} \tag{62}$$

This section introduces a straightforward and effective observer to estimate both the states and their derivatives, as well as the system disturbance in (62). To achieve this, the model in (62) can be reformulated as follows:

$$\dot{x} = Ax + Bu + d \tag{63}$$

where

$$A = \begin{bmatrix} -(\dfrac{1}{RC} + \dfrac{1}{r_C C}) & \dfrac{1}{C} \\ -\dfrac{1}{L} & -\dfrac{r_L}{L} \end{bmatrix}, \quad B = \begin{bmatrix} 0 \\ \dfrac{1}{L}V_{in} \end{bmatrix}$$
$$d = \begin{bmatrix} d_1 \\ d_2 \end{bmatrix} \tag{64}$$

Before introducing the observer, let us first consider the following theorem:

Theorem 2: For the given nonlinear system [44]-[45]

$$\begin{aligned} \dot{z}_1 &= z_2 \\ \dot{z}_2 &= L(z_1, z_2) \end{aligned} \tag{65}$$

If the system's output meets the criteria

$z_1(t), z_2(t) \to 0$ over time $t \to \infty$, then for $K, T > 0$ and any arbitrary input function $v(t)$ that is both bounded and integrable, the behavior of the resulting system will be as follows

$$\begin{aligned} \dot{x}_1 &= x_2 \\ \dot{x}_2 &= K^2 L(x_1 - v(t), x_2 / K) \end{aligned} \tag{66}$$

That fulfills the following equation:

$$\lim_{R\to\infty} \int_0^T |x_1 - v(t)| dt = 0 \tag{67}$$

This implies that $x_1(t)$ converge to $v(t)$.

Now, let's consider the following system with the parameters and variables defined in Theorem 2, whose asymptotic stability and convergence have been demonstrated in [46]. We are now prepared to present the general structure of the observer for the system (50) to estimate the state variables $x(t)$, as follows:

$$\begin{aligned} \dot{\hat{x}} &= Ax + Bu + \hat{d} \\ \dot{\hat{d}} &= K^2 L(\hat{x}_1 - x, \hat{d}/K) \end{aligned} \tag{68}$$

in which $\hat{x}$ and $\hat{d}$ are the estimated values of x and d, respectively. If the following holds

$$\lim_{R\to\infty} \int_0^T |\hat{x} - x| dt = 0 \tag{69}$$

The outcome, based on the first equation in (66) and using (61), is as follows:

Proof: As $R \to \infty$, the value $\left|\dot{\hat{d}}\right|$ tends to become unbounded, suggesting that the rate of change of $\hat{d}$ surpasses the rate at which $Ax + Bu$ changes. Furthermore, we obtain:

$$\begin{aligned} &\lim_{k\to\infty} \frac{d}{dt}\left\{Ax + Bu + \hat{d}\right\} = K^2 L(\hat{x}_1 - x, \hat{d}/K) \\ &\lim_{k\to\infty} \frac{Ax + Bu + \hat{d}}{K} = \frac{\hat{d}}{K} \end{aligned} \tag{70}$$

The outcome is that by replacing $Ax + Bu + \hat{d}$ with $x_2(t)$ in Theorem 2, the (68) and (69) hold true, thereby concluding the proof.

Remark 2. It should be noted that using the outputs of the State-disturbance Observer in (58) which are both estimating x as $\hat{x}$ and d as $\hat{d}$, the fractional-order adaptive sliding-mode control law in (27) is obtained as follows

$$u(t) = (G)^{-1}\left(-F - Y\hat{\theta} + \tau(t) + \hat{d}\right) \tag{71}$$

where τ and $\hat{\theta}$ are respectively obtained from (28) and (29), with the difference that wherever we used the output y, i.e. x_1 and also x_2 in sliding surface and controller equations, it is necessary to replace them with their estimates from the observer, i.e. $\hat{x}_1$ and $\hat{x}_2$. Now we can conclude that:

The Fast Finite Time Robust-Adaptive Fractional Order Sliding Mode Controller designed in this paper provides tracking of the output voltage in the DC-DC bulk converter in more realistic and applicable conditions where firstly all the dynamic parameters are unknown to the designer and secondly the bulk converter is exposed to unknown external disturbances and thirdly in senseless conditions or when, due to a sensor failure, the voltage and current values are not available in the feedback, they are estimated by the observer and provided to the controller. These are important achievements in the control of DC buck converters.

Remark 3 (Robustness)

The proposed controller in Theory 1 does not merely handle parameter *uncertainties* (e.g., ±20% variations in R/L), it solves the more realistic and more challenging problem of **complete parametric ignorance**. The adaptive law estimates the dynamic parameter vector θ (containing R, L, C, and so on) *without any prior knowledge of their values*. Also, the controller is robust against disturbances because the observer will compensate them for the controller as in (71). So, the controller's robustness stems from two key features:

1- **Adaptive Parameter Estimation**: The vector θ (containing R, L, and so on) is estimated online without requiring initial values, making the system inherently robust to any parameter uncertainty.
2- **Disturbance Observer:** Estimates d_1 and d_2 are actively canceled, handling both external disturbances and unmodeled dynamics.

Some Practical Implementation Advantages

The practical implementation of the proposed controller considers three key power electronics constraints: First, the duty cycle is directly derived from the control law through PWM conversion at the power stage's switching frequency. Second, the fractional-order operators are implemented digitally using the Oustaloup recursive approximation, optimized for real-time execution. Third, the adaptive laws are designed with projection operators to ensure parameter estimates remain within physically meaningful ranges (e.g., positive L, C values). This implementation maintains the theoretical guarantees while being computationally feasible for standard digital controllers.

Simulation Results

In this section, a hands-on example is offered to validate the performance of the proposed finite-time

sliding-mode fractional-order controller. The dynamic characteristics of the DC-DC converter used in this study are summarized in Table 1.

Table 1: Parameters of the DC-DC Converter for Simulation

Description	Quantity /Unit
Inductor (L)	1.8 *mH*
Inductor resistance (rL)	0.02 Ω
Capacitor (C)	0.0022 F
Capacitor resistance (rc)	1000 Ω
DC Load	25 Ω
Input voltage	240 V
Output Desired Voltage	100 V

A computational model is constructed, and a DC-DC buck converter is selected for performance assessment in this section. It is presumed that external disturbances are introduced into the system dynamics as follows:

$$\begin{aligned} &d_1(t) = 4, \quad 4 < t < 5 \\ &d_1(t) = 0, \quad others \\ &d_2(t) = 3, \quad 6 < t < 9 \\ &d_2(t) = 0, \quad others \end{aligned} \tag{72}$$

Next, the control parameters in (25) are determined as follows, based on the conditions established in Theorem 1:

$$\begin{aligned} &\alpha = 0.8, \quad \beta = 0.99, \quad \lambda = 0.8 \\ &\rho = 1500, \quad \mu = 1000, \\ &\Gamma = 50 I_5, \quad F = 0.5, \; G = 4 \end{aligned} \tag{73}$$

The simulation outcomes, which integrate the chattering mitigation strategy outlined in (49)-(50) and adopt the function $\sigma(t)$ as specified below, are demonstrated in the subsequent section.

$$\sigma(t) = \frac{1}{1+t^3} \tag{74}$$

The trajectory deviations of the converter's output voltage are depicted in Fig. 2 and Fig. 3. These visual representations validate that, despite system uncertainties and external perturbations, the converter's output voltage effectively tracks the reference signal within a finite duration of under 2 seconds. Moreover, the converter current remains constrained during the entire convergence phase.

The sliding surfaces shown in Fig. 4 confirm the anticipated finite-time convergence to zero. A closer inspection of the graph highlights the occurrence of chattering in the sliding mode. Nevertheless, implementing the chattering suppression strategy significantly reduces these oscillations. Moreover, the introduction of a fault influences these surfaces.

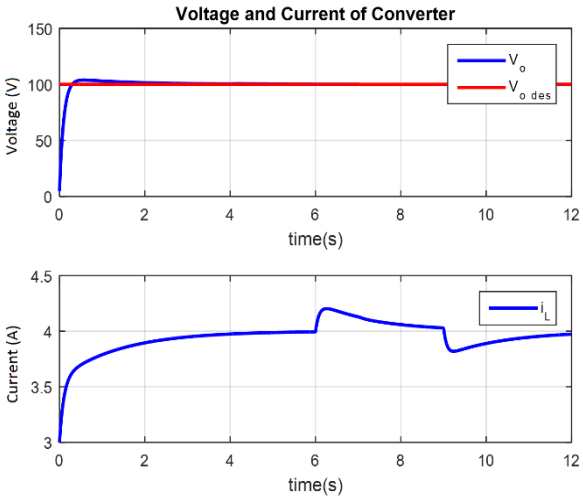

Fig. 2: Voltage and Current of DC-DC converter.

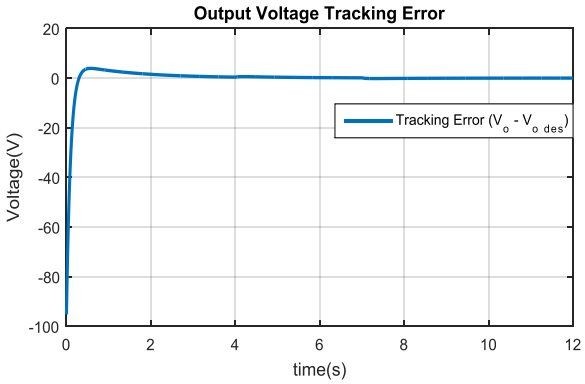

Fig. 3: Output voltage error of DC-DC Converter.

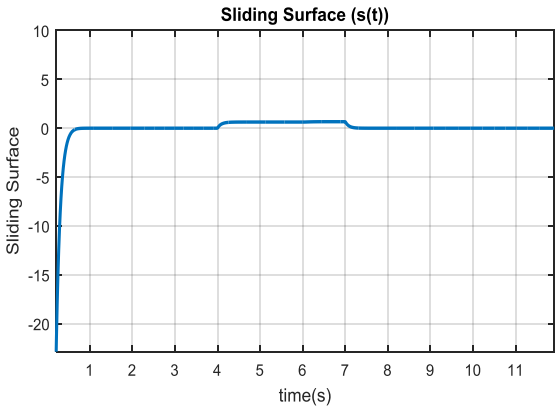

Fig. 4: Finite-time convergence of sliding surfaces utilizing chattering suppression technique.

Despite model uncertainties and external disturbances, the sliding surfaces achieve convergence to zero within a finite duration of less than 1 second, signifying the reaching phase. Once the surfaces reach zero, the system enters the sliding phase, leading to a gradual reduction in error values until complete convergence within the finite time demonstrated in Fig. 2 and Fig. 3.

According to the input signal characteristics displayed in Fig. 5, these values are regulated to hover around a unity mean, representing the discrete control input for the converter. Furthermore, the input signal exhibits negligible undesirable variations resulting from chattering.

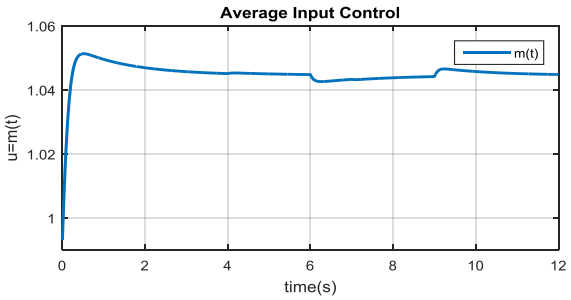

Fig. 5: Input signal of the bulk converter utilizing chattering reduction technique.

Fig. 6 and Fig. 7 illustrate the performance of the state observer. As shown in Fig. 6, and more clearly in the zoomed-in version of Fig. 7, both the output voltage and current of the converter are accurately estimated by the state observer within a fraction of a second.

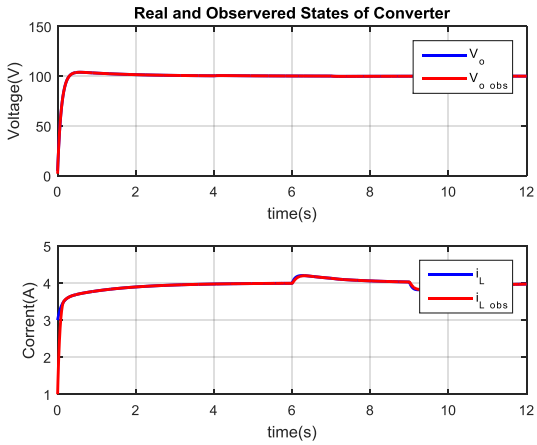

Fig. 6: Output of the observer for estimating the converter's state variables.

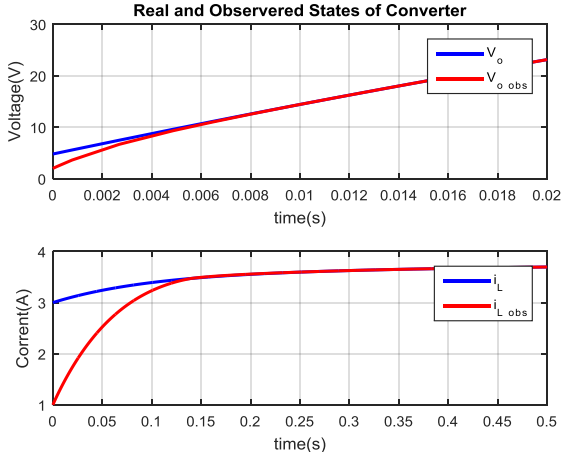

Fig. 7: Zoom in for: Output of observer for estimating the converter states.

Fig. 8 depicts the estimation errors of voltage and current by the observer.

This figure demonstrates the convergence of the state observer output error within a finite duration of approximately 0.1 seconds.

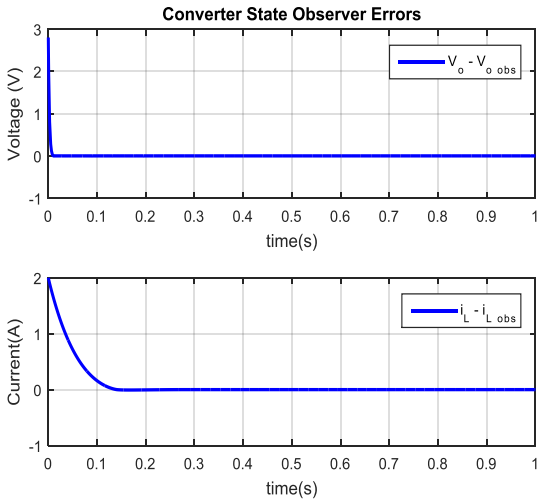

Fig. 8: Output errors of the observer for voltage and current

Fig. 9 illustrates the disturbance estimation, clearly indicating that the method for identifying and estimating external disturbances, as discussed in the previous section, has successfully estimated both voltage and current disturbances in the DC-DC buck converter. In addition to the amplitude, the method also accurately forecasts the disturbance's time of occurrence. Fig. 10 shows the disturbance estimation errors based on Fig. 9. As depicted, the error is nonzero only at the start and end of the disturbance, while during other intervals, the estimation error remains zero.

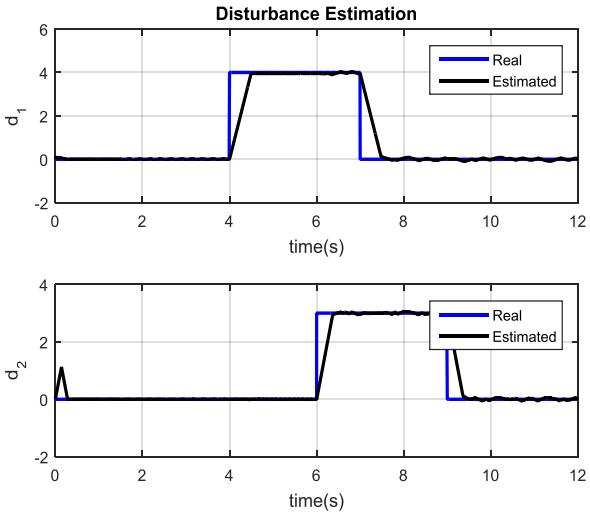

Fig. 9: Disturbance estimation using state-disturbance observer.

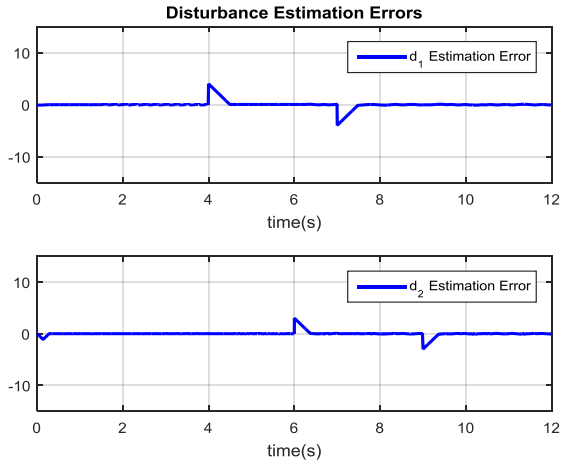

Fig. 10: Disturbance estimation errors.

Fig. 11 presents the dynamic estimation parameters resulting from the adaptive law. These parameters have reached well-defined finite limits, as anticipated. This outcome corroborates the stability of the adaptive law implemented by the controller.

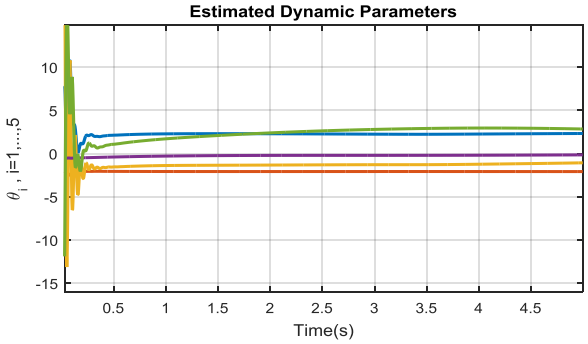

Fig. 11: Adaptive parameters of converter dynamic model.

The comprehensive simulation results demonstrate the successful performance of the fractional-order finite-time sliding mode control law in achieving the desired output convergence of the step-down DC–DC converter within a finite time. Moreover, the converter's unknown dynamic parameters are precisely identified through the adaptive mechanism, while the observer consistently estimates both the converter's voltage and current, along with the external disturbance. These outcomes confirm the precision and efficacy of the designed finite-time control law and its observer.

Comparison Results and Discussion

In [47], a control law employing a fractional-order sliding-mode approach for power converters utilizing a second-order state-space model is introduced, which bears resemblance to the method discussed in this thesis. In that study, the sliding mode control law is initially formulated by defining the sliding surface as shown below:

$$s = \alpha x_1^{\beta} + {}_{t_0}D_t^{\mu-1}x_2, \tag{75}$$

Ultimately, the control input necessary to stabilize the converter is derived, and its stability is proven as follows:

$$u(t) = \left[\frac{x_2}{RC} - D_t^{1-\mu}(\alpha\beta x_1^{\beta-1}x_2)\right]\frac{LC}{V_{in}} + \frac{(V_{ref}+x_1)}{V_{in}} - Ksign(s) - Ks \tag{76}$$

The parameters, along with their corresponding constraints, are as follows:

$$\begin{aligned} &\mu \in (0,1], \\ &\beta = q/p, \quad 0<\beta<1 \\ &0<q/p<1, \\ &K>0 \end{aligned} \tag{77}$$

Fig. 12 displays the simulation results of the control law presented in [47], in comparison with the finite-time sliding mode control law approach based on bounded disturbance estimation introduced in this paper. The disturbance is modeled with an increase in both its amplitude and magnitude, as detailed:

$$F_a = \begin{pmatrix} f_{a1} \\ f_{a2} \end{pmatrix}$$
$$f_{a1} = \begin{cases} 5 & for\ 4 \le t \le 7 \\ 0 & otherwise \end{cases} \tag{78}$$
$$f_{a2} = \begin{cases} 6 & for\ 6 \le t \le 9 \\ 0 & otherwise \end{cases}$$

The simulation results, which evaluate the buck converter's voltage and current responses using the dynamically identified parameters, clearly illustrate, as shown in Fig. 12, that while the time-bounded sliding mode control law from the referenced article is applied, the output response of the converter using that approach is less effective compared to the design proposed in this paper. The control law developed in this study demonstrates a considerable improvement in performance, especially in terms of the speed of output convergence to the desired value and the magnitude of the current.

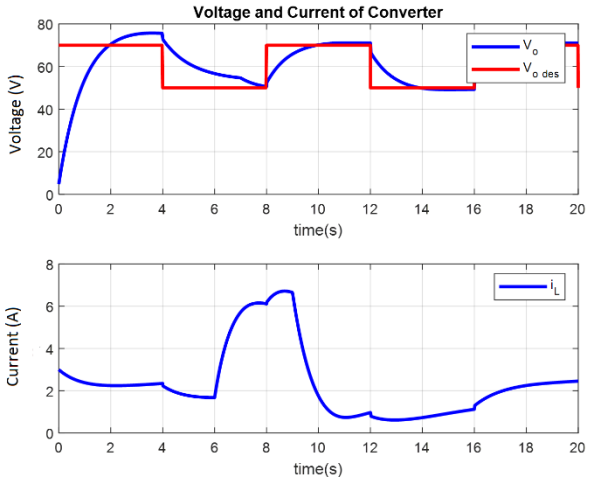

(a)

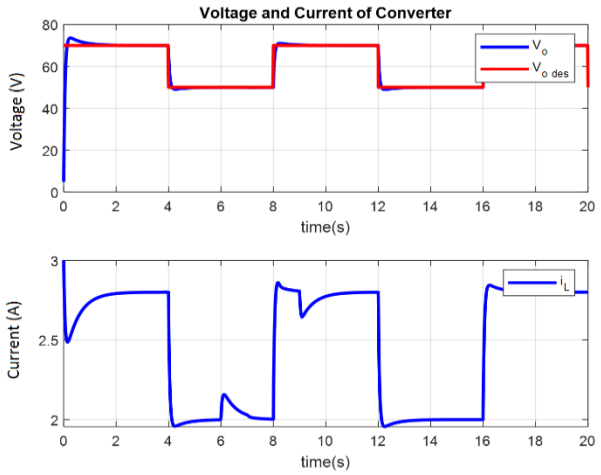

(b)

Fig. 12: Voltage and current of the DC-DC converter: (a) using the method proposed in [47], and (b) using the controller proposed in this work.

Enhanced Robustness Analysis

To rigorously validate the controller's robustness against parameters mismach, we tested its performance under ±20% parametric deviations in load resistance (R) and inductance (L) — two critical parameters that directly affect converter dynamics. These variations represent:

1-Load resistance (R) changes: Simulating sudden load steps (e.g., from 25Ω to 30Ω or 20Ω).

2-Inductance (L) variations: Modeling core saturation or manufacturing tolerances (1.8mH ±20%).

As it is clear from Fig. 13, the output voltage (V_o) converges to the reference (V_o desired) within 0.39 s for +20% R and 0.4 s for -20% R. Also, Overshoot remains below 15% in all cases, demonstrating the adaptive law's ability to compensate for unknown load changes without re-tuning. About Inductance Sensitivity (Fig. 13b – L Variations), Worst-case settling time is 0.36 s (+20% L), showing only a 9% delay vs. nominal. Also, the Overshoot remains less than 12% that is near to nominal value case.

As conclusion, the adaptive mechanism successfully compensates for ±20% parameter variations as shown in Table 2. The worst-case performance occurs with +20% Load resistance variation, showing only 16% degradation in Overshoot that is near to nominal case, while maintaining the finite-time convergence property.

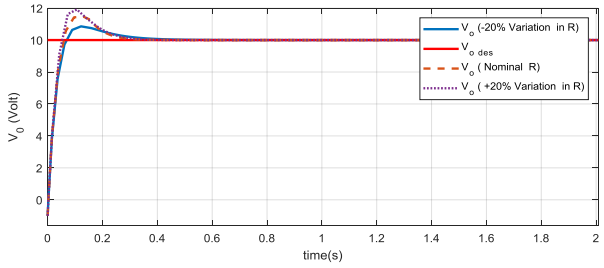

(a)

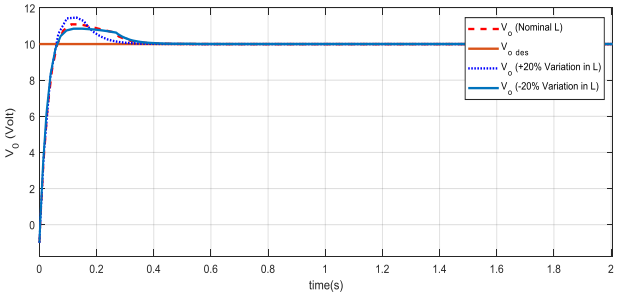

(b)

Fig. 13: Output voltage in Enhanced Robustness Analysis under: (a) load resistance variations, (b) Inductance variations.

Table 2:. Quantitative Insights in parameter mismatch robustness

Parameter	Variation	Settling Time (s)	Overshoot (%)
R (Load)	+20%	0.36	16
R (Load)	-20%	0.4	9
L	+20%	0.36	12
L	-20%	0.35	11

Closed-Loop System Overview

At the end of this section, Fig. 14 presents the complete control system block diagram proposed in the previous section to achieve finite-time stability in sensorless DC-DC bulk converters, considering that the dynamic parameters such as resistance and inductances are unknown and the external disturbances exist.

The proposed control architecture integrates four core components working in harmony. The state-disturbance observer continuously reconstructs the unmeasurable inductor current and unknown disturbances using only the output voltage, feeding these estimates to both the controller and adaptive law. Simultaneously, the adaptive parameter estimator adjusts the converter's unknown electrical parameters in real-time, ensuring accurate model compensation despite operating uncertainties.

These estimates dynamically tune the fractional-order sliding surface, which synthesizes the error dynamics using a unique blend of traditional and fractional calculus terms to enable smooth yet rapid convergence. The controller then combines all inputs - the sliding surface output, observer estimates, and adaptive parameters - to generate the precise PWM duty cycle that drives the converter while actively rejecting disturbances.

Signal Flow and Interactions

As shown in the Fig. 14, the system forms an intelligent closed loop where each block's outputs strategically inform the others.

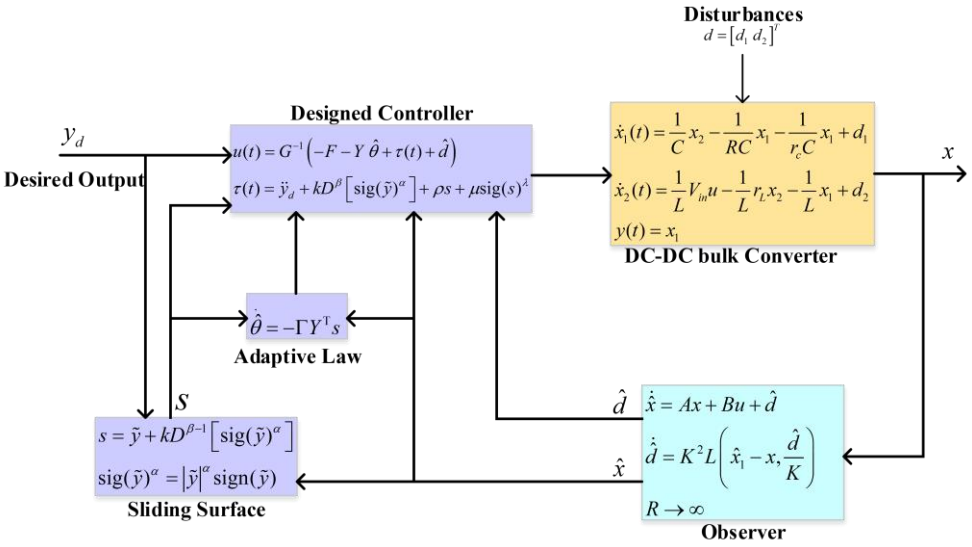

Fig. 14: Block Diagram of the Closed-Loop System.

The observer's state and disturbance estimates correct the controller's actions while also guiding parameter adaptation. Meanwhile, the sliding surface's fractional-order terms create a phase-advanced error signal that preemptively counters converter nonlinearities. This synergistic design achieves sensorless operation, robust disturbance rejection, and finite-time voltage regulation without requiring current measurements or offline calibration, as demonstrated in the simulation results.

Conclusion

This research presents an innovative controller based on fractional-order sliding mode control to achieve finite-time stability in DC-DC buck converters. A novel rapid‑convergent fractional‑order adaptive sliding-mode controller is introduced, ensuring the converter's output voltage attains the prescribed trajectory within a predetermined time span, even though none of the converter's dynamic parameters are known. A robust adaptive scheme is employed to uncover the converter's hidden circuit parameters. Additionally, a modern technique is proposed to minimize chattering in the sliding mode controller. To further improve the system's performance, a state‑disturbance observer is integrated to estimate both external disturbances and converter state variables, particularly in the event of sensor failures. Simulation results validate the effectiveness of the proposed method, demonstrating that the controller successfully smooths control actions, enhances the robustness of the DC-DC converter against model parameter uncertainties and disturbances, and guarantees the finite-time convergence of the output voltage to its desired value.

This work advances power electronics control by solving a previously unaddressed practical challenge: guaranteeing finite-time voltage regulation under complete parametric ignorance and missing sensor data. The controller's architecture provides inherent advantages for real-world applications, including automatic adaptation to component aging (through online parameter estimation), fault-tolerant operation (via state observation), and predictable worst-case performance (through finite-time convergence proofs). These features make the approach particularly suitable for mission-critical applications where reliability and deterministic performance are paramount, such as in aerospace power systems or medical equipment power supplies. Future work will focus on hardware validation and optimization for low-cost microcontroller implementations.

Author Contributions

S. R. Mousavi-Aghdam chose the field of research. M. Pourhasan collected information in this field. S. R. Mousavi-Aghdam presented the proposed structure. M. Pourhasan simulated and controlled the proposed converter structure in MATLAB software. The authors discussed the obtained results and drew conclusions. Under the supervision of S. R. Mousavi-Aghdam, the text of the article was prepared by M. pourhasan. S. R. Mousavi-Aghdamuploaded the article.

Acknowledgment

I appreciate the referees and their colleagues who helped the authors in publishing this article.

Funding

This research received no external funding.

Conflict of Interest

The authors declare no potential conflict of interest regarding the publication of this work. In addition, the

ethical issues including plagiarism, informed consent, misconduct, data fabrication and, or falsification, double publication and, or submission, and redundancy have been completely witnessed by the authors.

Abbreviations

ESB	Extended State Observer
SMC	Sliding Mode Control
PID	Proportional Integral Derivative
PWM	Pulse Width Modulation
FOC	Fractional Order Control
FTDO	Finite Time Disturbance Observer

References

[1] Z. Qi, M. B. Hossain, M. R. Islam, M. A. Rahman, R. Raad, "Advancement in converter topology, control, and power management: Magnetic linked power converter for emerging applications," IEEE Access, (12): 101228-101246, 2024.

[2] X. Li, J. Wang, A. Wang, "The transient power oscillation suppression for parallel grid-forming converters using the superconducting transmission," IEEE Trans. Appl. Supercond., 34(8): 1-5, 2024.

[3] T. R. Palleswari Yalla, A. Siva, K. P. Swaroopg, G. Durga Prasad, M. Deenakonda, R. Banothu, "Comprehensive analysis and performance investigation of non-isolated DC-DC converters in solar photovoltaic applications," in Proc. International Conference on Computational Intelligence for Green and Sustainable Technologies (ICCIGST): 1-6, 2024.

[4] R. Kushwaha, V. Khadkikar, A. Edpuganti, "Electric vehicle on-board fast charging through converter maximum switch utilization," IEEE Trans. Power Electron., 39(1): 998-1014, 2024.

[5] F. Ahmeti, S. Osmanaj, D. Arnaudov, "Comparative Analysis and Optimization Parallel Operation Strategies in DC-DC Converters for Smart DC Grid Integration," in Proc. 2024 International Conference on Renewable Energies and Smart Technologies (REST): 1-5, 2024.

[6] Z. Wang, S. Li, Q. Li, "Continuous nonsingular terminal sliding mode control of DC–DC boost converters subject to time-varying disturbances," IEEE Trans. Circuits Syst. II Exp. Briefs, 67(11): 2552-2556, 2020.

[7] S. Li, K. Yu, G. Zhang, S. W. Sin, X. Zou, Q. Zou, "Design of fast transient response voltage-mode buck converter with hybrid feedforward and feedback technique," IEEE J. Emerg. Sel. Top. Power Electron., 9 (1):780-790, 2021.

[8] S. Sharma, T. Aggarwal, V. Bisht, G. Kaushik, "Comparison of PID tuning methods for buck converter system," in Proc. 2024 IEEE Third International Conference on Power Electronics, Intelligent Control and Energy Systems (ICPEICES): 132-136, 2024.

[9] Q. Zhang, R. Wang, T. Wang, Y. Huo, "Research on parameter self-tuning method of PI controller for DC-DC converters based on energy conversion mechanism," in Proc. IEEE Transportation Electrification Conference and Expo, Asia-Pacific (ITEC Asia-Pacific): 380-385, 2024.

[10] L. Cavanini, G. Cimini, G. Ippoliti, A. Bemporad, "Model predictive control for pre-compensated voltage mode controlled DC-DC converters," IET Control Theory Appl., 11(15): 2514-2520, 2017.

[11] A. Garcés-Ruiz, S. Riffo, C. González-Castaño, C. Restrepo, "Model predictive control with stability guarantee for second-order DC/DC Converters," IEEE Trans. Ind. Electron., 71(5): 5157-5165, 2024.

[12] Z. Liu, L. Xie, A. Bemporad, S. Lu, "Fast Linear parameter varying model predictive control of buck DCDC converters based on FPGA," IEEE Access, (6): 52434-52446, 2018.

[13] H. Wang, Z. Zhang, C. Y. Weng, X. Tang, "Robust finite-time control for DC–DC buck converter with inductor current constraint," IEEE Trans. Ind. Electron., 71(8): 9631-9638, 2024.

[14] J. Fei, D. Jiang, "Fuzzy neural network sliding-mode controller for DC-DC buck converter," IEEE Internet Things J., 11(19): 31575-31586, 2024.

[15] X. Wang et al., "Adaptive voltage-guaranteed control of DC/DC-buck-converter-interfaced DC microgrids with constant power loads," IEEE Trans. Ind. Electron., 71(11): 14926-14936, 2024.

[16] Y. Zhang, C. Tang, Y. Zheng, X. Tang, K. Nang Leung, "An adaptive zero-current detector for single-inductor multiple-output DC-DC converter with full-wave current sensor," IEEE Trans. Very Large Scale Integr. (VLSI) Syst., 32(9): 1764-1768, 2024.

[17] X. Wang et al., "Adaptive voltage-guaranteed control of DC/DC-buck-converter-interfaced DC microgrids with constant power loads," IEEE Trans. Ind. Electron., 71(11): 14926-14936, 2024.

[18] R. Sureshkumar, S. Ganeshkumar, "Comparative study of proportional untegral and backstepping controller for buck converter," in Proc. International Conference on Emerging Trends in Electrical and Computer Technology: 375-379, 2011.

[19] J. Yang, H. Cui, S. Li, A. Zolotas, "Optimized active disturbance rejection control for DC-DC buck converters with uncertainties using a reduced-order GPI observer," IEEE Trans. Circuits Syst. I: Regul. Pap., 65(2): 832-84, 2018.

[20] D. Montoya-Acevedo, W. Gil-González, O. D. Montoya, C. Restrepo, C. González-Castaño, "Adaptive speed control for a DC motor using DC/DC converters: An inverse optimal control approach," IEEE Access, 12: 154503-154513, 2024.

[21] Y. Shtessel, C. Edwards, L. Fridman, A. Levant, Sliding Mode Control and Observation, New York, NY:Springer New York, 2014.

[22] J. Wang, S. Li, J. Yang, B. Wu, Q. Li, "Extended state observer-based sliding mode control for PWM-based DC-DC buck power converter systems with mismatched disturbances," IET Control Theory Appl., 9(4): 579-586, 2021.

[23] H. Lin, Y. Yin, J. Liu, L. Wu, L. Franquelo, "Extended state observer based second order sliding mode control strategy for DC-DC buck converters," in Proc. IEEE International Conference on Electrical Machines and Systems: 1-6, 2019.

[24] J. Wang, S. Li, J. Yang, B. Wu, Q. Li, "Finite-time disturbance observer based non-singular terminal sliding mode control for pulse width modulation based DC-DC buck converters with mismatched load disturbances," IET Power Electron., 9(9): 1995-2002, 2016.

[25] T. Waghmare, P. Chaturvedi, "A higher-order sliding mode controller's super twisting technique for a DC–DC converter in photovoltaic applications," Energy Rep., 9(10): 581-589, 2023.

[26] S. Huerta-Moro, O. Martínez-Fuentes, V. R. Gonzalez-Diaz, E. Tlelo-Cuautle, "On the sliding mode control applied to a DC-DC buck converter," Technologies, 11(2): 33, 2023.

[27] J. Fei, X. Gong, "Self-organizing fuzzy neural nonsingular fast terminal sliding mode control of DC-DC buck converter," IEEE Trans. Circuits Syst. I: Regul. Pap., 71(9): 4309-4322, 2024.

[28] M. Veysi, M. R. Soltanpour, "Voltage-base control of camera stabilizer using optimal adaptive fuzzy sliding mode control," J. Iran. Assoc. Electr. Electron. Eng., 14(4): 23-40, 2018.

[29] B. Yodwong, D. Guilbert, W. Kaewmanee, M. Phattanasak, M. Hinaje, G. Vitale, "Improved sliding mode-based controller of a high voltage ratio DC–DC converter for electrolyzers supplied by renewable energy," IEEE Trans. Ind. Electron., 71(8): 8831-8840, 2024.

[30] I. Chairez, V. Utkin, “Electrocardiographically signal simulator based on a sliding mode controlled buck DC-DC power converter,” IFAC-PapersOnLine, 55(9): 419-424, 2022.

[31] J. Lu, M. Savaghebi, Y. Guan, J. C. Vasquez, A. M. Y. M. Ghias, J. M. Guerrero, "A reduced-order enhanced state observer control of DC-DC buck converter," IEEE Access, (6): 56184-56191, 2018.

[32] M. Score, "Ceramic or electrolytic output capacitors in DC/DC converters," Analog Appl. J., 2015.

[33] G. Shahabadi, M. Naseh, S. Es'haghi, “A new method for sliding mode controller design and parameters selection in DC-DC Z-source converter," J. Iran. Assoc. Electr. Electron. Eng., 20(2): 183-194, 2023.

[34] A. Arian, M. Yazdani, "An interleaved switching buck converter with soft switching condition," J. Iran. Assoc. Electr. Electron. Eng., 18(4):19-29, 2021.

[35] X. Chen, G. Liu, "Sensorless optimal commutation steady speed control method for a nonideal back-EMF BLDC motor drive system including buck converter," IEEE Trans. Ind. Electron., 67(7): 6147-6157, 2020.

[36] L. Liu, W. X. Zheng, S. Ding, "An adaptive SOSM controller design by using a sliding-mode-based filter and its application to buck converter," IEEE Trans. Circuits Syst. I Reg. Papers, 67(7): 2409-2418, 2020.

[37] M. Naderi Soorki, M. S. Tavazoei, "Fractional-order linear time invariant swarm systems: Asymptotic swarm stability and time response analysis," Cent. Eur. J. Phys., 11(6): 845-854, 2013.

[38] Y. H. Youssri, “Orthonormal ultraspherical operational matrix algorithm for fractal–fractional riccati equation with generalized caputo derivative,” Fractal and Fractional, Special Issue: Numerical Methods and Simulations in Fractal and Fractional Problems, 5(3): 100: 1-11, 2021.

[39] M. N. Soorki, T. V. Moghaddam, A. Emamifard, "A new fast finite-time fractional-order adaptive sliding-mode control for a quadrotor," in Proc. 7th International Conference on Control, Instrumentation and Automation (ICCIA): 1-5, 2021.

[40] Y. Wang, L. Gu, Y. Xu, et al., “Practical tracking control of robot manipulators with continuous fractional-order nonsingular terminal sliding mode,” IEEE Trans. Ind. Electron., 63(10): 6194-6204, 2016.

[41] S. P. Bhat, D. S. Bernstein, “Finite-time stability of continuous autonomous systems,” SIAM J. Control Optim., 38(3): 751-766, 2000.

[42] E. Cruz-Zavala, J. A. Moreno, L. Fridman, Lyapunov-based design for a class of variable-gain 2nd-sliding controllers with the desired convergence rate,” Int. J. Robust Nonlinear Control, 28(17): 5279-5296, 2018.

[43] N. Soorki, M. S. Tavazoei, “Adaptive robust control of fractional-order systems in the presence of model uncertainties and external disturbances,” IET Control Theory Appl., 12(7): 961-969, 2018.

[44] X. Wei Bu, X. Yan Wu, Y. Xing Chen, R.Y. Bai, “Design of a class of new nonlinear disturbance observers based on tracking differentiators for uncertain dynamic systems,” Int. J. Control Autom. Syst., 13(3): 1-8, 2015.

[45] J. Q. Han, W. Wang, “Nonlinear tracking differentiator,” J. Syst. Sci. Math. Sci., 14(2): 177-183, 1994.

[46] G. Y. Qi, Z. Q. Chen, Z. Z. Yuan, “New tracking-differentiator design and analysis of its stability and convergence,” J. Syst. Eng. Electron., 15(4): 780-787, 2004.

[47] N. Yang, et al., "Fractional-order terminal sliding-mode control for buck DC/DC converter," Math. Probl. Eng., 2016: 1-7, 6935081, 2016.

Biographies

Seyyed Reza Mousavi-Aghdam received his M.Sc. and Ph. D. Degree from University of Tabriz, Iran, in 2011 and 2015 respectively all in Electrical Engineering. During September 2014 to March 2015, he has been a Visiting Research Scholar at the Department of Industrial Engineering, University of Padova, Italy. In 2016, he joined the Department of Electrical Engineering, University of Mohaghegh Ardabili, as an Assistant Professor. Since 2020, he has been an Associate Professor of Electrical Engineering. His activity deals with the design and control of electrical machines using FEM, electric drives and converters. He is the author or coauthor of several scientific papers on electrical machines and drives. His current research interests include design and control of electrical machines and electric drives.

- Email: R.mousaviaghdam@uma.ac.ir
- ORCID: 0000-0002-0154-4427
- Web of Science Researcher ID: V-3336-2019
- Scopus Author ID: 355001780700
- Homepage: https://academics.uma.ac.ir/profiles?Name=S.%20R.%20Mousavi-Aghdam

Milad Pourhasan was born in Ardabil, Iran, on April, 1997. He received M.Sc. degree in Electrical Control Engineering from of University of Mohaghegh Ardabili in Ardabil, Iran. He is currently pursuing the Ph.D. degree in the Electrical Engineering at University of Mohaghegh Ardabili in Ardabil, Iran. His research interests include electric vehicle and power electronics design, simulation, modeling, and control of electrical machines.

- Email: milad.pur1996@gmail.com
- ORCID: 0009-0007-5280-7403
- Web of Science Researcher ID: NA
- Scopus Author ID: NA
- Homepage: NA